N87-26021

EXPERIENCE WITH 3-D COMPOSITE GRIDS*

J. A. Benek, T. L. Donegan, and N. E. Suhs
Calspan Corporation/AEDC Division

ABSTRACT

Experience at the AEDC with the three-dimensional (3-D), chimera grid embedding scheme is described. Applications of the inviscid version to a multiple-body configuration, a wing/body/tail configuration and an estimate of wind tunnel wall interference are described. Applications to viscous flows include a 3-D cavity and another multi-body configuration. A variety of grid generators is used, and several embedding strategies are described.

1.0 INTRODUCTION

In the last ten years, Computational Fluid Dynamics (CFD) has evolved from an interesting spectator sport into a necessary, if not integral, part of aircraft design and development. Two circumstances have stimulated this change: the maturation of fast numerical algorithms for solution of the Euler and Navier-Stokes equations and the reduction of the price of the large supercomputers required to perform the computations. As the entry costs decrease and the value of flow simulations becomes more widely recognized, the demands for ever more complex simulations increase. The heightened level of expectation also increases pressure to produce "timely" solutions. This pressure can only be expected to increase as CFD becomes more closely coupled to the design and development processes. Frequently, the most critical phase in meeting the demand for computations is the construction of a suitable mesh. To ameliorate the difficulties experienced with grid generation, alternative computational strategies are being explored. Basically, they can be divided into two categories: global approaches and domain decomposition approaches.

The global mesh approach uses a single computational net to discretize the geometry and flow field [e.g., Thompson (1982), Rubbert and Lee (1982), and Shang and Scherr (1985)]. Complex geometry frequently requires the introduction of internal boundaries (e.g., cuts) into the domain and may result in very skewed grids and regions of unacceptably low spatial resolution. The introduction of internal boundaries increases the bookkeeping required in the flow solver and can require modifications to the solution algorithm. One novel approach utilizing a global mesh is described by Jameson, Baker, and Weatherhill (1986). The major thrust of this work is to use a finite volume algorithm based on tetrahedrons and eliminate the requirement for an ordered mesh. More data structure is required to define the relationships among the grid points comprising the volumes.

Domain decomposition includes many techniques: zonal or grid patching [e.g., Hessenius and Pulliam (1982), Rai (1984), and Holst et al. (1985)], and grid embedding/oversettings [e.g., Atta and Vadyak (1982), Benek et al. (1983), Venkatapathy and Lombard (1985), and Berger (1982)]. The basic idea of this strategy is the subdivision of the computational domain into regions (not necessarily disjoint) that can be more easily meshed. An additional advantage is that each subdomain may be treated separately and a different flow model or solution algorithm used in each. Such flexibility provides economies in computer resources as the more expensive viscous flow solvers can be confined to regions where viscosity dominates the flow. The key to successfully implementing this strategy is provision of a means of intergrid communication. This is the point at which the various techniques differ most widely. All these techniques require additional bookkeeping to facilitate communication.

Presently, no one method has been demonstrated to be clearly superior. It seems likely that some synthesis of the various strategies will become the method of choice. In the meantime, we have chosen the grid-embedding approach as it includes grid patching as a special case and thus provides a flexible method for accomplishing a broad range of flow simulations. In this paper we will describe our experience with the chimera scheme which was first developed by Benek, Steger and Dougherty (1983). The three-dimensional, color graphics code required to support this effort was developed by Buning and Steger (1985).

2.0 DESCRIPTION

The chimera grid-embedding technique is a domain decomposition strategy and as such has two principal elements: (1) decomposition of the domain into subdomains which typically overlap and (2) communication among the subdomains. The division into subdomains is arbitrary; the major considerations are the identification of regions that may be easily meshed, and perhaps the isolation of special regions of the flow (e.g., where viscous effects are important). The chimera implementation increases the flexibility of subdomain selection by removing regions of a mesh common to an embedded grid. That is, an embedded mesh introduces an artificial boundary or "hole" into the mesh in which it is embedded, figure 1. Because the regions interior to the hole do not enter into the solution process, intergrid communication is simplified since communication among the grids is restricted to the transfer of boundary data. Appropriate boundary values are interpolated from the mesh or meshes in

*The research reported herein was performed by the Arnold Engineering Development Center (AEDC), Air Force Systems Command. Work and analysis for the research were done by personnel of Calspan Corporation/AEDC Division, operating contractor for the AEDC aerospace flight dynamics test facilities. Further reproduction is authorized to satisfy needs of the U. S. Government.

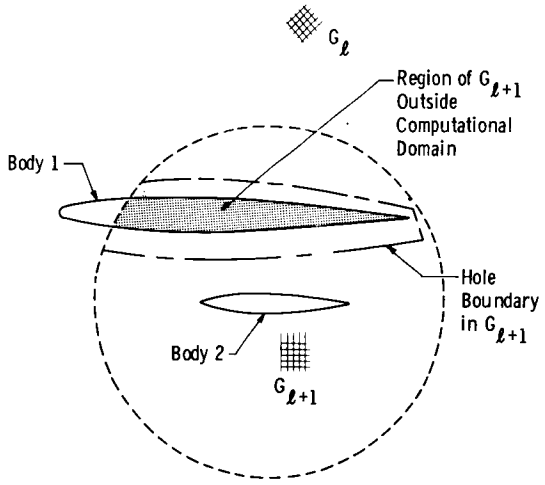

Figure 1. Hole boundary in embedded grid $G_{\ell+1}$ caused by solid boundary in G_ℓ.

which the boundary is embedded. The chimera procedure naturally separates into two parts, (1) generation of the composite mesh and associated interpolation data and (2) solution of the flow model or models on each mesh. Each part is embodied in a separate computer code, PEGSUS and XMER3D. PEGSUS takes independently generated component or subdomain grids and the embedding specifications as input and automatically constructs the composite mesh and computes the interpolation data which are output. XMER3D takes the PEGSUS output and flow specifications as input and solves the appropriate flow model on each grid.

2.1 PEGSUS

Automatic generation of a composite mesh from the input component grids requires PEGSUS to (1) establish the proper lines of communication among the grids through appropriate data structure, (2) construct holes within grids, (3) identify points within holes, (4) locate points from which boundary values can be interpolated, and (5) evaluate interpolation parameters. In addition, PEGSUS performs consistency checks on the interpolation data to assure their acceptability and constructs output files with the data structures appropriate to XMER3D. The most recent version of PEGSUS allows very general interactions among grids as indicated in figure 2. In addition, any grid may introduce a hole into any other mesh. Details of the hole construction process, and associated data structures, are provided by Benek et al. (1983, 1985, and 1986). A trilinear interpolation is used to obtain boundary data.

2.2 XMER3D

The implementation of the chimera scheme must provide for the use of multiple flow models. The current choice of models is the 3-D Euler equations for inviscid flow and the 3-D thin-layer Navier-Stokes equations for viscous flow. The algebraic model of Baldwin/Lomax (1978) is used to simulate turbulent flow. The implicit, approximate factorization scheme of Beam and Warming (1976 and 1977) is used to solve the model equations. The implementation follows that of Pulliam and Steger (1978) and uses explicit boundary conditions. Modifications to accommodate the chimera scheme are described by Benek et al. (1986).

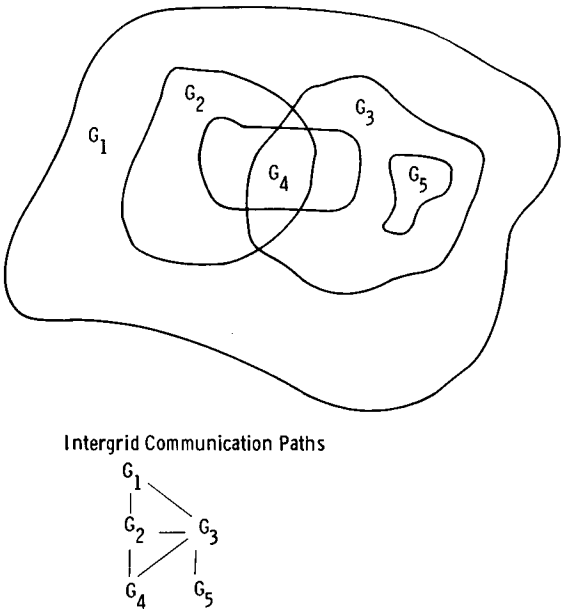

Figure 2. Structure of embedded grids.

3.0 APPLICATIONS

A major motivation for the development of the chimera scheme at the AEDC was the requirement to provide routine computational support to testing. Estimates of the effects of the wind tunnel environment on aerodynamic data are of particular interest. Typically, lead times are short and grid generation is usually the pacing item in performing CFD simulations. Also, there is the requirement to compute time-dependent flows involving aerodynamic configurations in relative motion as exemplified by the Space Shuttle booster configuration and store separation from military aircraft.

The 3-D chimera scheme has been used to compute both viscous and inviscid flows over a variety of configurations. These include wing/body/tail, bodies in close proximity, cavity flows, and base flows for Mach numbers spanning the range from subsonic to supersonic. The following sections will illustrate some of these applications of the chimera scheme.

3.1 Inviscid Flows

The flow about a three-body configuration (fig. 3) consisting of three ellipsoidal bodies in a triangular arrangement was computed for a free-stream Mach number, $M_\infty = 0.8$, and angle of attack, $\alpha = -2.0$ deg. The composite mesh contained three grids and 57,750 points. The component grids were constructed using a hyperbolic grid generator described by Steger and Chaussee (1980) and Kinsey and Barth (1984). Mach number contours are shown in figure 4. The contours indicate that the expected symmetries exist in the flow.

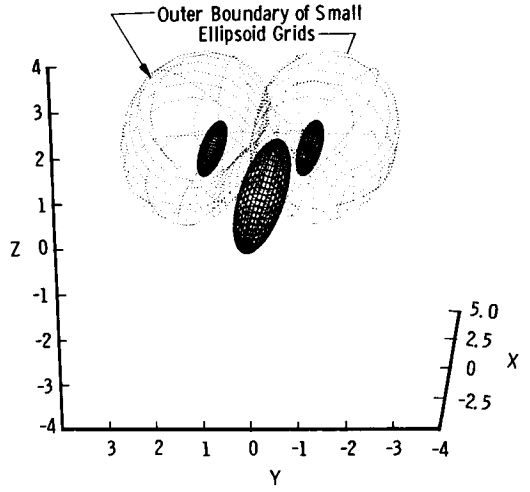

Figure 3. Three-ellipsoid-body configuration and grids.

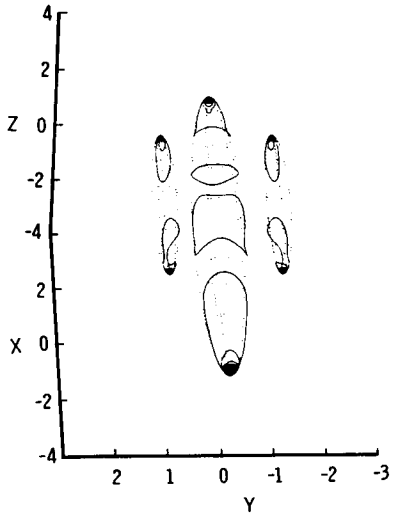

Figure 4. Mach number contours on surfaces of ellipsoids, $M_\infty = 0.80$, $\alpha = -2$ deg.

One of the intended uses of the chimera scheme at the AEDC is the computation of wind tunnel wall and support interference [e.g., Kraft et al. (1986) and Suhs (1985)]. A version of the scheme was converted to this purpose. The model shown in figure 5 was designed for assessment of wind tunnel wall interference and it consists of a blunted ogive-cylinder and a mid-mounted wing and tail. The wing and tail are constant chord planforms swept back at 30 deg and have no twist or taper. Cross sections parallel to the plane of symmetry are NACA-0012 airfoils. Figure 6 illustrates the meshes used to represent the wall interference model shown in figure 5. The wind tunnel walls and a portion of the sting support are also represented. Figure 6 shows the outer boundaries of the grids about the fuselage, wing, and tail; figure 7 illustrates the model embedded in the tunnel mesh. The region devoid of mesh lines on the tunnel symmetry plane in figure 7 represents the hole in the tunnel grid introduced by excluding points in the vicinity of the model from the solution in the tunnel grid.

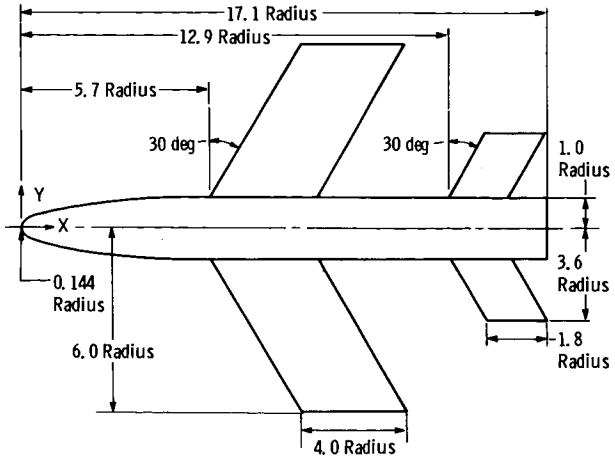

Figure 5. Wing/body/tail configuration.

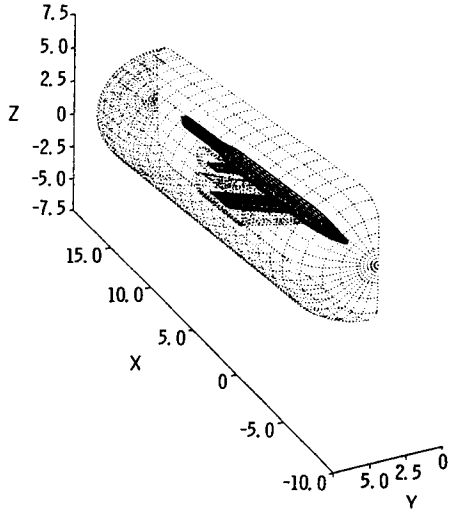

Figure 6. Composite grid for fuselage, sting, wing, and tail grids.

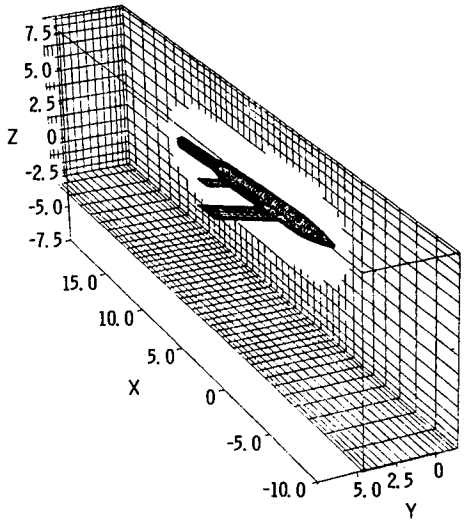

Figure 7. Model grids embedded in the tunnel grid.

Figure 7 illustrates the flexibility inherent in the chimera scheme. The model geometry and sting grids were constructed by adding a mesh containing the sting to an existing mesh used to model the fuselage. The component-by-component construction process is particularly useful for wall interference calculations because no additional grid generation is required to change model angle of attack. All that is required is that the grids representing the wind tunnel model be rotated relative to the tunnel mesh and be re-embedded in it. PEGSUS performs such transformations on component grids by a single change of input.

Figure 8 illustrates the component grids used to represent a generic transport configuration for a wall interference assessment. In this case, three grids containing a total of 201,000 points are used.

Several grid generators were used to construct the component grids shown in figures 6 through 8. These include a two-dimensional grid generator developed by Sorenson (1980) and the three-dimensional generators developed by Soni (1985) and Thompson (to be published in 1987).

Mach number contours on the wall interference model are presented in figure 9 [Benek et al. (1985 and 1986)]. The tunnel solution obtained on the grids shown in figures 6 and 7 corresponds to $M_\infty = 0.90$ and $\alpha = 4$ deg. The contours join smoothly across mesh boundaries. The shock wave on the wing can be seen to continue around the fuselage. The figure illustrates the effect of decreasing spatial resolution in high gradient regions. The shock wave can be seen to be smeared on the fuselage compared to the wing because of the decreased resolution in the fuselage grid. Figure 10 [Benek et al. (1985)] presents a comparison of computed and measured wing and fuselage pressure coefficients for $M_\infty = 0.9$ and $\alpha = 2$ deg. The solution corresponds to an interference-free flow on a composite mesh with 157,540 points. Details of wall interference computations will be presented at the AIAA 19th Fluid Dynamics, Plasma Dynamics and Laser Conference, June 1987.

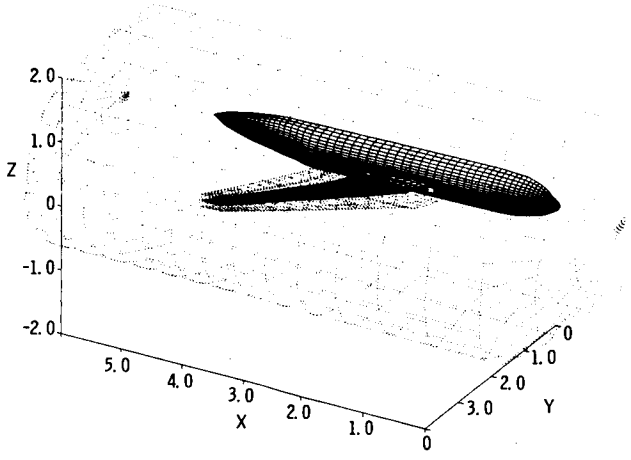

Figure 8. Fuselage and body grids for a transport configuration.

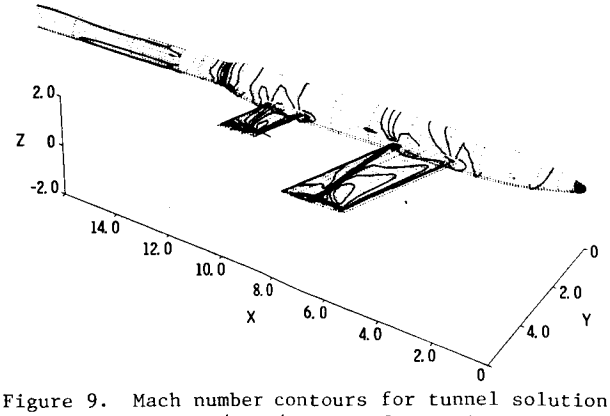

Figure 9. Mach number contours for tunnel solution of wing/body/tail configuration, $M_\infty = 0.9$, $\alpha = 4$ deg.

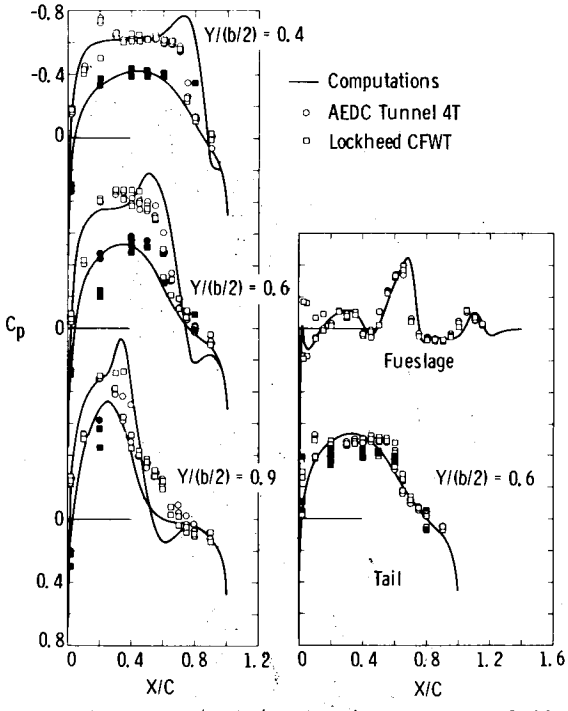

Figure 10. Wing/body/tail solution, $M_\infty = 0.90$, $\alpha = 2$ deg (open symbols, upper surface; solid symbols, lower surface).

3.2 Viscous Flows

The chimera scheme was used to compute several 3-D viscous flows: cavity flow, the flow about a three-body configuration and the flow about a blunt-based projectile. The cavity flow simulation is time-dependent because of the fluctuating free shear layer over the cavity. The cavity has a length-to-depth ratio of 5.6 and a length-to-width ratio of 3.35. Figure 11 illustrates the composite mesh used to represent the cavity/flat-plate flow field. The composite mesh has two grids, a total of 157,627 points, and no holes. The component grids are stretched cartesian nets with clustering near the solid boundaries and in the shear layer. Figure 12 presents computed Mach number contours in the streamwise plane of symmetry for $M_\infty = 0.74$. The contours correspond to the flow at a single instant of time. The three-dimensional nature of the flow is demonstrated in figure 13 which shows the flow in a plane normal to the stream direction and located half way down the cavity. Details of this computation and additional solutions will be presented at the AIAA 19th Fluid Dynamics, Plasma Dynamics and Laser Conference in June 1987.

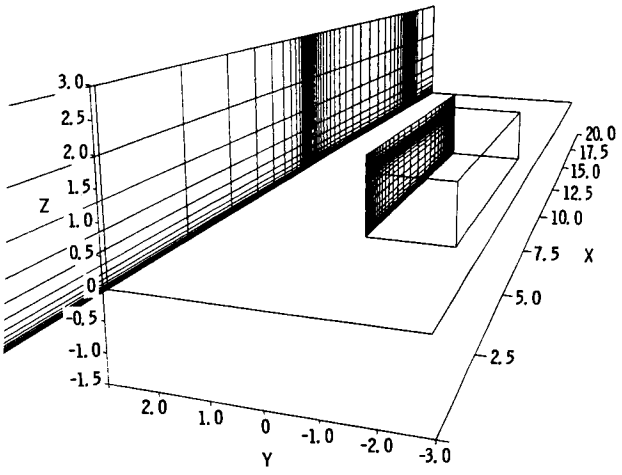

Figure 11. Composite mesh for a cavity flow.

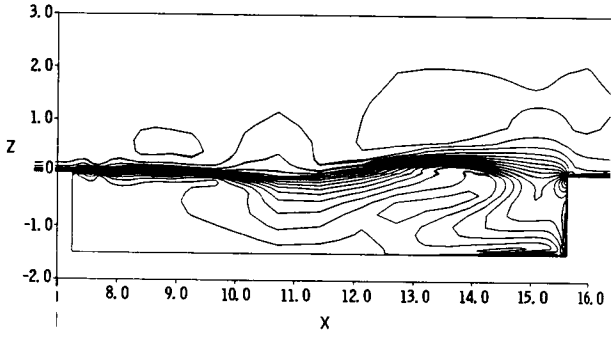

Figure 12. Symmetry plane Mach number contours, $M_\infty = 0.74$.

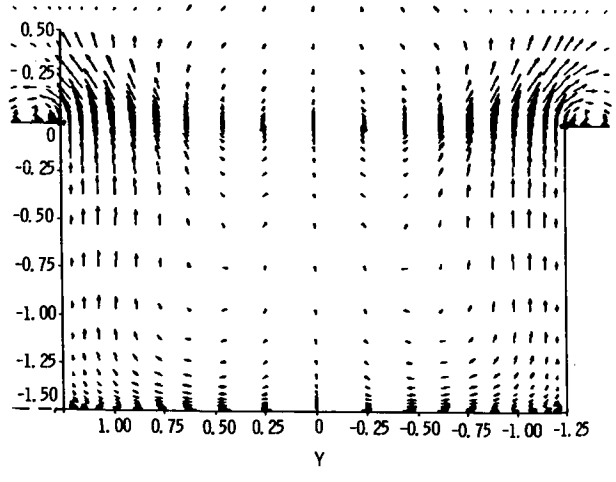

Figure 13. Cross flow vector vectors at center of cavity for $M_\infty = 0.74$.

The flow about a configuration of three bodies in close proximity was computed. Figures 14 and 15 show the structure of the composite grid. Seven component grids with 496,216 points represent the flow field. Each body has a single viscous grid and is embedded in a cylindrical mesh which has been segmented into three overlapping sections. A hemispherical mesh surrounds the entire configuration Figure 15 shows a projection of the grids onto the symmetry plane of the lower body in figure 14 and illustrates the overlaps among the component grids. The composite mesh shows a range of grid interactions: patching among grids, e.g., G_2, G_3 and G_4, hole production by grids, e.g., G_5, G_6, G_7 in meshes G_2, G_3, and G_4, and holes crossing grid boundaries, e.g., G_5 across G_2, G_3, and G_4. Detailed comparisons of computations and experimental data at several transonic Mach numbers and angles of attack will be presented at the 8th AIAA Computational Fluid Dynamics meeting in June 1987.

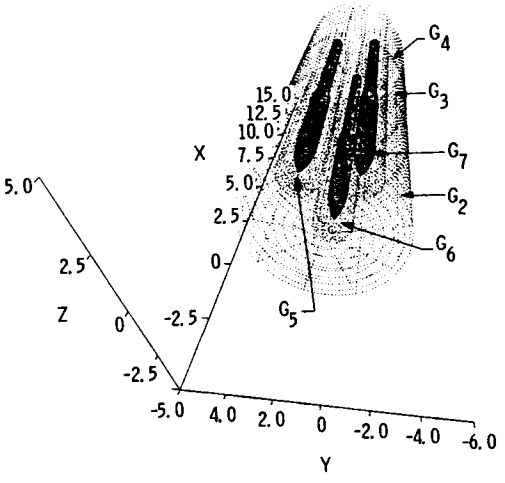

Figure 14. Multiple bodies in close proximity.

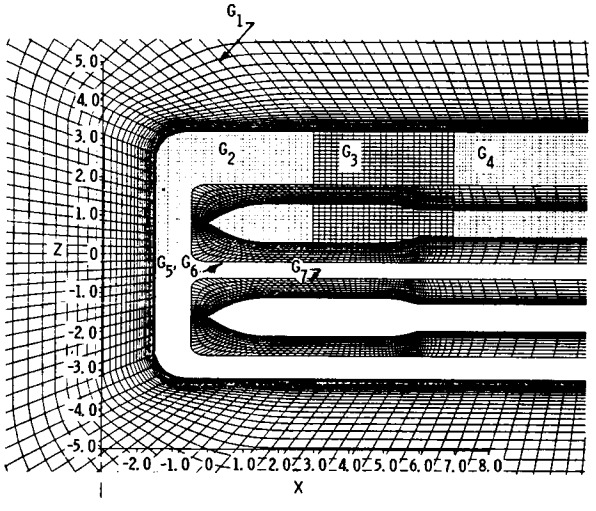

Figure 15. Projection of grids for multiple body configuration in symmetry plane of G_7.

The final example is the flow about a blunt-based projectile. The composite mesh shown in figure 16 consists of two "patched" grids containing a total of 68,000 points. This flow is being examined as part of a sting interference study. A comparison of computed and measured pressure coefficients [Kayser and Whiton (1982)] is given in figure 17 for the transonic flow conditions of $M_\infty = 0.91$ and $\alpha = 0$ deg. Comparisons of experimental and predicted values of base pressure are also in good agreement. Additional computations on similar configurations are being made.

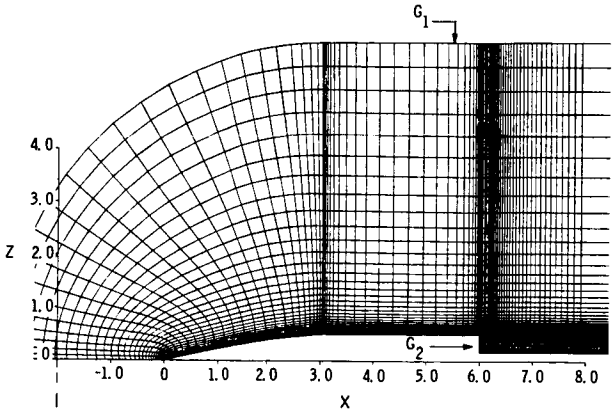

Figure 16. Composite mesh for blunt-based projectile.

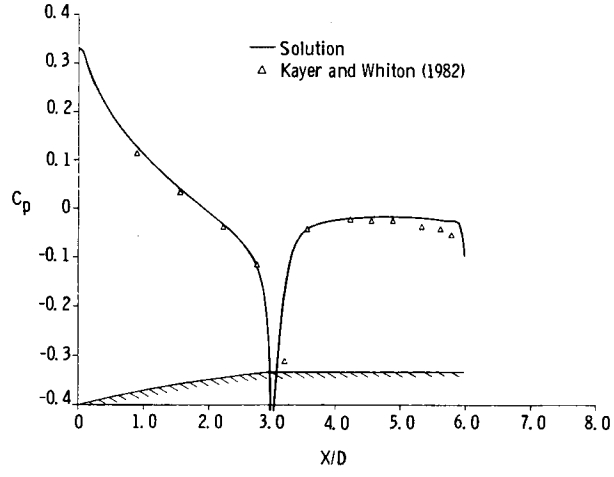

Figure 17. Comparison of computed and measured pressure coefficients for blunt-based projectile, $M_\infty = 0.91$, $\alpha = 0$ deg.

4.0 DISCUSSION

Sections 2 and 3 described our experience with the chimera scheme. However, there are several other aspects of its use that cannot be as clearly documented and several questions remain unanswered. Perhaps, the most significant change that was made from the two-dimensional (2-D) work reported by Benek et al. (1983) was a change from the mixed 2nd/4th-order accurate approximations of Pulliam and Steger (1978) to a consistently 2nd-order approximation. Large oscillations in the solution with the mixed-order scheme occurred when grid boundaries crossed high gradient regions. Switching to a 2nd-order scheme has eliminated this problem.

Another question that commonly arises involves the interpolation at grid boundaries. Is the boundary approximation conservative? Our experience indicates that the major factor affecting accuracy at the boundaries is the resolution between the grids in the neighborhood of the boundary. Whenever there is a "large" mismatch in resolution, convergence slows and large oscillations in the solution are evident near the interface. Should the mismatch occur where the interface crosses a high gradient region, the situation is exacerbated. A more detailed and systematic study of this aspect of domain decomposition techniques is in order.

SUMMARY

We have described our experience with the chimera grid-embedding scheme. The method was applied to the computation of transonic wall interference with particular success and is being used routinely for support to testing at the AEDC. Experience with the viscous version is still being accumulated, but the potential to compute a wide range of flows has been demonstrated. Component grids have been generated by several two- and three-dimensional grid codes which employ algebraic and partial differential equations as generators. We experienced no difficulties combining grids constructed by the various methods into a composite mesh.

REFERENCES

Atta, E. H.; and Vadyak, J. A.: A Grid Interfacing Zonal Algorithm for Three-Dimensional Transonic Flows About Aircraft Configurations, AIAA Paper No. 82-1017, June 1982.

Baldwin, B. S.; and Lomax, H.: Thin Layer Approximation and Algebraic Model for Separated Turbulent Flows, AIAA Paper No. 78-257, January 1978.

Beam, R.; and Warming, R. F.: An Implicit Finite Difference Algorithm for Hyperbolic Systems in Conservation Law Form, Journal of Computational Physics, vol. 22, no. 1, September 1976, pp. 87-110.

Beam, R.; and Warming, R. F.: An Implicit Factored Scheme for Compressible Navier-Stokes Equations, AIAA Paper No. 77-645, June 1977.

Benek, J. A.; Steger, J. L.; and Dougherty, F. C.: A Flexible Grid Embedding Technique with Application to Euler Equations, AIAA Paper No. 83-1944, July 1983.

Benek, J. A.; Buning, P. G.; and Steger, J. L.: A 3-D Chimera Grid Embedding Technique, AIAA Paper No. 85-1523, July 1985.

Benek, J. A.; Steger, J. L.; Dougherty, F. C.; and Buning, P. G.: Chimera: A Grid Embedding Technique, AEDC-TR-85-64 (AD-A167466), April 1986.

Berger, M. J.: Adaptive Mesh Refinement for Hyperbolic Partial Differential Equations, Stanford University STAN-CS-82-924, August 1982.

Buning, P. G.; and Steger, J. L.: Graphics and Flow Visualization in Computational Fluid Dynamics, AIAA Paper No. 85-1507, July 1985.

Hessenius, K. A.; and Pulliam, T. H.: A Zonal Approach to Solutions of the Euler Equations, AIAA Paper 82-0969, June 1982.

Holst, T. L.; Kaynak, U.; Gundy, K. L.; Thomas, S.D.; Flores, J.; and Chaderjian, N. M.: Numerical Solution of Transonic Wing Flows Using an Euler/Navier-Stokes Zonal Approach, AIAA Paper No. 85-1640, July 1985.

Jameson, A.; Baker, T. J.; and Weatherhill, N. P.: Calculation of Inviscid Transonic Flow over a Complete Aircraft, AIAA Paper No. 86-103, January 1986.

Kayser, L. D.; and Whiton, F.: Surface Pressure Measurements on a Boattailed Projectile Shape at Transonic Speeds, U. S. Army Ballistic Research Laboratory, Aberdeen Proving Ground, Maryland, ARBRL-MR-03161, March 1982.

Kinsey, D. W.; and Barth, T. J.: Description of a Hyperbolic Grid Generating Procedure for Arbitrary Two-Dimensional Bodies, AFWAL TM 84-91, FIMM, July 1984.

Kraft, E. M.; Ritter, A.; and Laster, M. L.: Advances at AEDC in Treating Transonic Wind Tunnel Wall Interference, Presented at the 15th Congress, International Council of the Aeronautical Sciences, London, UK, September 1986.

Pulliam, T. H.; and Steger, J. L.: On Implicit Finite Difference Simulations of Three-Dimensional Flows, AIAA Paper No. 78-10, January 1978.

Rai, M. M.: A Conservative Treatment of Zonal Boundaries for Euler Equation Calculations, AIAA Paper 84-0164, January 1984.

Rubbert, P. E.; and Lee, K. D.: Patched Coordinate Systems, Numerical Grid Generation, J. F. Thompson, ed., North-Holland, New York, NY, 1982.

Shang, J. S.; and Scherr, S. J.: Navier-Stokes Solution of the Flow Field Around a Complete Aircraft, AIAA Paper 85-1509, July 1985.

Soni, B. K.: Two and Three-Dimensional Grid Generation for Internal Flow Applications of Computational Fluid Dynamics, AIAA Paper No. 85-1526, July 1985.

Sorenson, R. L.: A Computer Program to Generate Two-Dimensional Grids About Airfoils and Other Shapes by Use of Poisson's Equations, NASA TM 81198, May 1980.

Steger, J. L.; and Chaussee, D.: Generation of Body Fitted Coordinates Using Hyperbolic Partial Differential Equations, SIAM Journal on Scientific and Statistical Computing, vol. 1, December 1980, pp. 431-437.

Suhs, N. E.: Computational Estimates of Strut Support Interference at Transonic Mach Numbers, AIAA Paper No. 85-5018, October 1985.

Thompson, J. F., ed.: Numerical Grid Generation. North-Holland, New York, NY, 1982.

Thompson, J. F.: A Composite Grid Generation Code for General 3-D Regions, AIAA Paper No. 87-275 (to be published).

Venkatapathy, E.; and Lombard, C. K.: Flow Structure Capturing on Overset Patch Meshes, AIAA Paper No. 85-1690, July 1985.